Lacosamide Derivatives with Anticonvulsant Activity as Carbonic Anhydrase Inhibitors. Molecular Modeling, Docking and QSAR Analysis

Juan C. Garro Martinez[*,1,2], Esteban G. Vega-Hissi[1], Matías F. Andrada[1], Pablo R. Duchowicz[3], Francisco Torrens[4] and Mario R. Estrada[1]

[1]*Area de Química Física, Facultad de Química, Bioquímica y Farmacia, Universidad Nacional de San Luis, Chacabuco 917, San Luis, 5700, Argentina*

[2]*Centro Científico Tecnológico San Luis (CCT-CONICET), Facultad de Química, Bioquímica y Farmacia, Universidad Nacional de San Luis, Chacabuco 917, San Luis, 5700, Argentina*

[3]*Instituto de Investigaciones Fisicoquímicas Teóricas y Aplicadas (INIFTA, UNLP, CCT La Plata-CONICET), Diag. 113 y 64, Sucursal 4, C.C. 16, 1900 La Plata, Argentina*

[4]*Institut Universitari de Ciència Molecular, Universitat de València, Edifici d'Instituts de Paterna, València, Spain*

Abstract: Lacosamide is an anticonvulsant drug which presents carbonic anhydrase inhibition. In this paper, we analyzed the apparent relationship between both activities performing a molecular modeling, docking and QSAR studies on 18 lacosamide derivatives with known anticonvulsant activity. Docking results suggested the zinc-binding site of carbonic anhydrase is a possible target of lacosamide and lacosamide derivatives making favorable *Van der Waals* interactions with Asn67, Gln92, Phe131 and Thr200. The mathematical models revealed a poor relationship between the anticonvulsant activity and molecular descriptors obtained from DFT and docking calculations. However, a QSAR model was developed using Dragon software descriptors. The statistic parameters of the model are: correlation coefficient, R=0.957 and standard deviation, S=0.162. Our results provide new valuable information regarding the relationship between both activities and contribute important insights into the essential molecular requirements for the anticonvulsant activity.

1. INTRODUCTION

The compound lacosamide, simply appointed as LCM, is successfully marketed in the United States and Europe for the adjunctive treatment of partial-onset seizures in adults [1, 2]. This novel anticonvulsant drug was synthesized for the first time by Kohn *et al.* in 1996 [3]. Afterwards, several studies on biological activity of LCM derivatives were presented in the literature [4-9]. The proposed anticonvulsant mechanism suggests that LCM modulates inactivating the gate sodium channels and the collapsin response mediator protein [10-12]. In addition, other authors hypothesize that carbonic anhydrase (CA) might be a putative target for this interesting compound [13, 14]. The CA is a zinc-containing enzyme which catalyzes a simple physiological reaction, the interconversion between carbon dioxide and bicarbonate ion. Thus, the CA takes part in important physiological processes connected with respiration and transport of CO_2/bicarbonate between metabolizing tissues and the lungs. Investigations affirm that anticonvulsant effect of carbonic anhydrase inhibitors is due to retention of CO_2 to inhibition of the red cell and brain enzymes [15, 16]. The Zn(II) is coordinated by three histidine (His) and a water molecule or a hydroxide ion

which acts as nucleophile in the conversion reaction [17-19]. The presence of this metal is critical for the catalytic cycle of the enzyme, however, a possible inhibitory mechanism in which LCM does not interact with the Zn(II) is showed by literature [14]. The rationale for studying of LCM as CA inhibitor is based on the following evidence: (a) several anticonvulsants, such as topiramate and zonisamide show potent CA inhibition, (b) the shape of lacosamide and known CA inhibitors have similar features, i.e., an aromatic ring and a hydroxypentyl-type extended side chain [20, 21].

In a previous report [22], we performed a multivariable QSAR analysis on a library of 51 LCM derivatives extracted from several bibliographies [2-10]. We demonstrated the more important role of electronic and topologic features of compounds on their anticonvulsant activity in relative to constitutional parameters. Despite the information, there is little data in the literature concerning the interactions between LCM and derivatives with CA into the action site. In addition, the essential molecular requirements of (R)-LCM, enantiomer defined as the active isomer on the voltage-gated sodium channels [12-14], associated to both activities are not clearly established.

The main objective of the research presented in this paper is to explain the chemical and molecular features necessary for CA inhibition and the anticonvulsants activity, as well as analyze the connection between both activities [14, 19, 23]. For this propose, a data set including (R)-LCM and 18

*Address correspondence to this author at the Area de Química Física, Facultad de Química, Bioquímica y Farmacia, Universidad Nacional de San Luis, Chacabuco 917, San Luis, 5700, Argentina; Tel/Fax: (54) 266 4423789, Ext. 122; E-mail: jcgarro@unsl.edu.ar

derivatives with well-known activity was screened as possible CA inhibitors through molecular docking studies. Also, we performed new mathematical relationships between the experimental activity and molecular descriptors obtained from density function theory (DFT) optimizations and molecular docking calculations. Finally, an original linear QSAR model was developed using the calculated molecular descriptors in combination with Dragon software descriptors [24].

2. MATERIALS AND METHODS

2.1. Biological Experimental Data

The experimental anticonvulsant activity of the data set was extracted from the studies of Salomé *et al*. [10]. This data set was selected even when other authors report the activity of several LCM derivatives [2-10]. Thus, we make sure that anticonvulsant activity was determined in identical experimental conditions and a regular distribution of data is obtained, even if it means a small number of compounds. The activity expressed as ED_{50} (dose of chemical compound for which the 50% of the individuals reaches the desired effect) was converted into $Log_{10}ED_{50}$ and used as the independent variable in the QSAR analysis. The chemical

structures, ED_{50} and $Log_{10}ED_{50}$ values of the studied compounds are listed in Table **1**.

2.2. Geometry Optimizations

Twenty four different possible conformations of LCM were evaluated in gas and condensed phase (solvent) by means of *ab initio* (Hartree Fock) and DFT (B3LYP) calculations with 6-31+G(d) basis set [25-27]. All calculations in condensed phase were performed employing the integral equation formulation of the polarizable continuum model (IEF-IPCM) [28, 29]. The most stable conformation of LCM was used as a backbone to make the starting structure for to optimize 18 LCM derivatives. We used Gaussian 09 to perform the quantum-mechanical calculations [30].

2.3. Molecular Docking

The software Autodock Vina [31] was used to perform the docking calculations. The crystal structure of the CA was obtained from Protein Data Bank [32] (PDB code: 3IEO [14]) and the only water molecule coordinating the Zn(II) was kept. All the remaining co-crystallized molecules were

Table 1. Total Energies (in Hartree) for Conformers of LCM in Gas and Condensed Phase

ID.	HF/ 6-31+G(d)	ΔE kcal mol^{-1}	B3LYP/ 6-31+G(d)	ΔE kcal mol^{-1}	IEF-PCM/ B3LYP/6-31+G(d)[a]	ΔE kcal mol^{-1}
1	-836.311148	0.00	-841.459605	0.00	-841.475400	0.00
2	-836.301109	6.30	-841.450213	5.89	-841.470271	3.21
3	-836.304189	4.36	-841.451545	5.05	-841.470787	2.89
4	-836.285423	16.14	-841.444804	9.28	-841.464636	6.75
5	-836.301741	5.90	-841.449726	6.19	-841.470103	3.32
6	Not Found					
7	-836.305619	3.47	-841.455008	2.88	-841.471783	2.27
8	-836.292044	11.98	-841.441412	11.41	-841.462619	8.02
9	-836.300117	6.92	-841.449142	6.56	-841.466241	5.74
10	Not Found					
11	-836.288987	13.90	-841.438055	13.52	-841.459954	9.69
12	Not Found					
13	-836.309490	1.04	-841.458220	0.86	-841.473748	1.03
14	-836.301206	6.23	-841.450666	5.60	-841.470132	3.30
15	-836.304700	4.04	-841.452117	4.69	-841.470815	2.87
16	Not Found					
17	-836.286972	15.17	-841.436888	14.25	-841.460651	9.25
18	-836.285105	16.34	-841.435141	15.35	-841.456683	11.74
19	Not Found					
20	Not Found					
21	Not Found					
22	-836.301694	5.93	-841.449726	6.19	-841.470103	3.32
23	Not Found					
24	-836.303850	4.58	-841.451907	4.83	-841.472049	2.10

[a] Dielectric constant of ε=78.39 (dielectric constant of water).

removed. The grid box was defined to include completely the proposed binding site and standard parameters for the docking calculation were used except for exhaustiveness for which a value of 100 was set.

2.4. Molecular Descriptors

The dipole moment, E_{HOMO}, E_{LUMO} and GAP energy obtained from optimization calculation at B3LYP/6-31+G(d) and the ΔG_{bind} calculated from molecular docking were used as molecular descriptors to asses interaction between these compounds and its receptor. Other descriptors have been employed previously on different biomolecular systems for the same purpose [33-35]. Besides, 1497 molecular descriptors were computed using the Dragon program [24] including all types of descriptors such as Constitutional, Topological, Geometrical, Charge, GETAWAY (Geometry, Topology and Atoms-Weighted AssemblY), WHIM (Weighted Holistic Invariant Molecular descriptors), 3D-MoRSE (3D-Molecular Representation of Structure based on Electron diffraction), Molecular Walk Counts, BCUT descriptors, 2D-Autocorrelations, Aromaticity Indices, Randic Molecular Profiles, Radial Distribution Functions, Functional Groups, Atom-Centered Fragments, Empirical and Properties [36].

Molecular descriptors with high correlation give redundant information. These descriptors were eliminated including only one of them to total set. Thus, 1210 descriptors gather enough information and redundant data are avoided.

2.5. Search and Validation of the QSAR Model

There are a great number of selection methods of best descriptors from a pool of variables. In earlier reports [37, 38], we used the replacement method (RM) that produces linear QSAR models that are quite close to the full search methods with lower computational cost [39, 40]. The RM is an efficient optimization tool which generates multiparametric linear QSAR models by searching an optimal subset of d descriptors from a set of D descriptors (d<<<D) with minimum standard deviation (S) of the model.

In order to verify the predictive capability of the QSAR relationships established, we choose the well-known leave-one-out (loo) and leave-more-out (l%o) cross-validation procedures where % represents the percentage of molecules removed from the calibration set. For the l % procedure, we generated 1000000 cases, with % = 20 (four compounds). Also, a rigorous and more realistic model validation procedure was applied. This consists in using an external set of molecules which do not form part of the calibration set. In addition, we applied the y-randomization approach (10000 cases of random scrambling) to establish model robustness and to demonstrate the best model was not found by chance [41]. This approach consists in exchange of the experimental property in such a way the property value and the compound do not match.
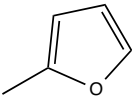
The computer system employed for all QSAR calculations was Matlab 7.0 [42].

3. RESULTS AND DISCUSSIONS

3.1. Conformational Analysis of LCM and Derivatives

The structures of the twenty four conformations of LCM are presented in Fig. (**1S**) of supplementary material. Table **1** lists the total electronic energies of the LCM conformers in the different levels of theory used. From most stable structure, conformer 1, the 18 LCM derivatives were generated and optimized at B3LYP/6-31+G(d) (Table **2**). The results suggest the optimized structures of LCM derivatives adopt a similar conformation with the most stable conformation of LCM, Fig. (**1**) illustrates the overlap of the conformations. Only the compounds 17, 18 and 19 have the aromatic ring in a different orientation. These compounds have a different substitute to CH_2OCH_3 in R^1 that can influence the conformation of the ring.

Table 2. Structure and Anticonvulsant Activity for LCM and Derivatives

ID	R^1	R^2	ED_{50} µM	Log_{10} ED_{50}
1 (LCM)	CH_2OCH_3	H	17.98	1.255
2	CH_2OCH_3	3-F	25.72	1.410
3	CH_2OCH_3	4-F	15.65	1.195
4	CH_2OCH_3	$4-OCF_3$	10.77	1.032
5	CH_2OCH_3	$4-CH_3$	41.61	1.619
6	CH_2OCH_3	$4-CH(CH_3)_2$	29.07	1.463
7	CH_2OCH_3	$4-CH_2OCH_3$	247.97	2.394
8	CH_2OCH_3	$4-(CH_2)_3OCH_3$	62.03	1.793
9	CH_2OCH_3	$4-CH=CH_2$	12.66	1.103
10	CH_2OCH_3	$4-C_6H_5$	24.51	1.389
11	CH_2OCH_3	$4-CCCH_2OCH_3$	31.41	1.497
12	CH_2OCH_3	4-CN	544.78	2.736
13	CH_2OCH_3	$4-N_3$	28.63	1.457
14	CH_2OCH_3	4-Cl	17.56	1.244
15	CH_2OCH_3	4-Br	26.43	1.422
16	CH_2OCH_3	4-I	42.53	1.629
17	CH_3	H	249.66	2.397
18	CH_2OH	H	224.29	2.351
19		H	12.12	1.083

3.2. Molecular Docking

The crystal structure of CA extracted from Protein Data Bank (PDB [31] code: 3IEO [14], resolution of 2.0 Å) presents a complex with (S)-LCM enantiomer. The authors
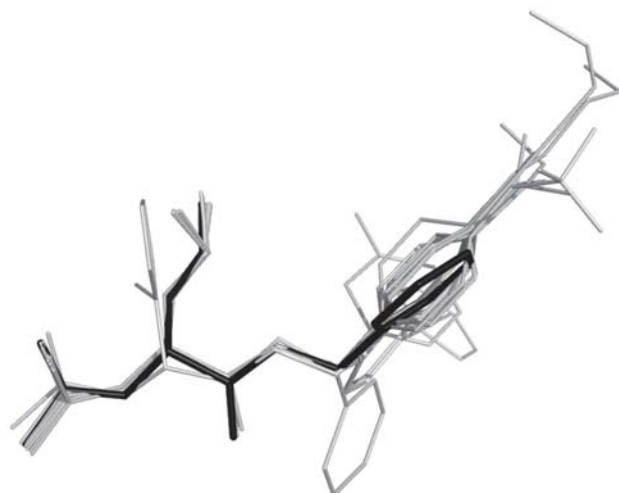
Fig. (1). Overlap of the most stable conformations of LCM (black) and derivatives (gray).

show that (S)-LCM interacts in the active site with Asn67, Gln92, Phe131 and Thr200 but no interactions with the Zn(II) were evidenced [14], see Fig. (**2**) (top and bottom left panels). We found that (R)-LCM adopts an extended conformation in the active site close to the amino acid Asn67, Gln92, Phe131 and Thr200, as indicate the bibliography [43, 44]. The docking performed to 18 LCM derivatives, Fig. (**2**) (bottom right panel), shows that these compounds bind to the active site of CA interacting with mentioned amino acid. Besides, the (R)-LCM and LCM derivatives have similar values of ΔG_{bind} (about -6.0 kcal mol^{-1}) indicating that LCM derivatives have an effective bind with the CA.

3.3. QSAR Models

In order to develop the most reasonable linear QSAR model, we used 15 compounds in the calibration set and 4 compounds in the test set (Table **3**). The elements of each set were selected in such a way that they share similar structural characteristics and the experimental data of the test set
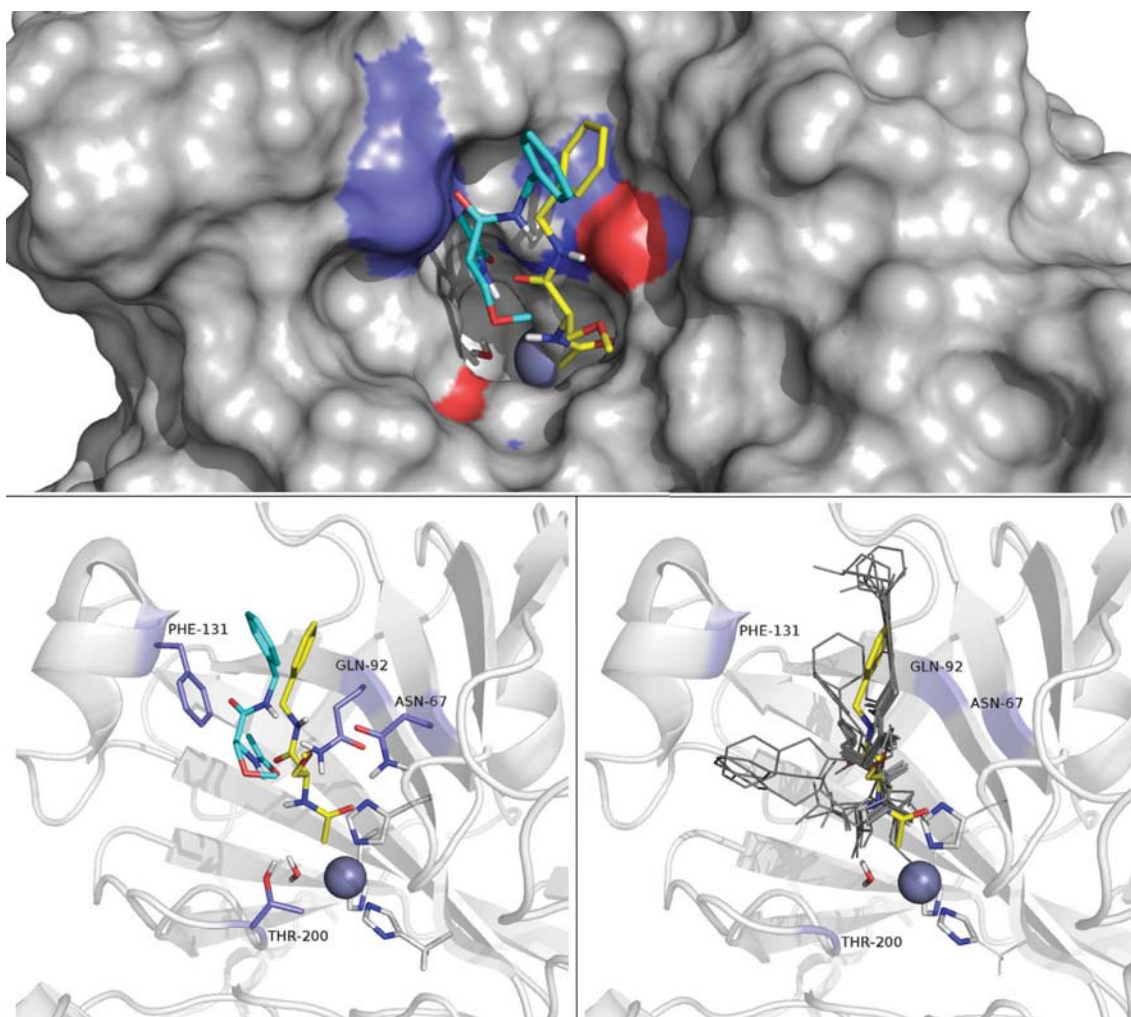

Fig. (2). The (S)-LCM, LCM and derivatives into the CA. Protein is represented as a gray surface (top panel) or cartoon (bottom panels) and Zn(II) ion and coordinated water molecule are shown as a blue sphere and sticks, respectively. Top panel. Comparison of the docked LCM (yellow sticks) and the co-crystallized (S)-LCM (cyan sticks) in the active site of CA. Interacting residues are highlighted in color. Bottom left panel. Interacting residues are shown in blue sticks. Bottom right panel. Superposition of LCM (yellow sticks) and derivatives (dark gray lines) into the active site.

Table 3.   Molecular Descriptors Calculated from DFT Calculation and Molecular Docking Study

ID	μ	E_{HOMO}	E_{LUMO}	GAP	ΔG_{bind} kcal mol^{-1}	MATS8p	nCN	Log$_{10}$ ED$_{50}$ Exp	Log$_{10}$ ED$_{50}$ Pred [a]
1	3.506	-0.2543	-0.0258	-0.228	-5.9	0.176	0	1.255	1.324
2	3.520	-0.2590	-0.0366	-0.22	-5.9	0.17	0	1.410	1.353
3*	1.920	-0.2556	-0.0337	-0.221	-5.7	0.169	0	1.195	1.357
4	4.119	-0.2616	-0.0406	-0.220	-6.2	0.211	0	1.032	1.157
5*	3.663	-0.2465	-0.0228	-0.223	-5.9	0.162	0	1.619	1.391
6*	3.665	-0.2460	-0.0218	-0.224	-6.3	0.239	0	1.463	1.023
7*	2.194	-0.2506	-0.0316	-0.218	-5.7	0.076	0	2.394	2.102
8	2.300	-0.2465	-0.0258	-0.220	-5.9	0.067	0	1.793	1.845
9	3.220	-0.2337	-0.0536	-0.180	-6	0.219	0	1.103	1.118
10	3.546	-0.2352	-0.0454	-0.189	-6.6	0.162	0	1.389	1.391
11	2.092	-0.2408	-0.0522	-0.188	-5.9	0.067	0	1.497	1.845
12	2.500	-0.2639	-0.0700	-0.193	-6.1	0.215	1	2.736	2.736
13	3.167	-0.2378	-0.0521	-0.185	-5.7	0.141	0	1.457	1.491
14	3.337	-0.2528	-0.0368	-0.215	-5.9	0.218	0	1.244	1.123
15	1.775	-0.2517	-0.0381	-0.213	-5.9	0.201	0	1.422	1.204
16	1.636	-0.2504	-0.0342	-0.216	-5.8	0.129	0	1.629	1.549
17	3.593	-0.2539	-0.0335	-0.220	-5.5	0.009	0	2.397	2.122
18	2.967	-0.2527	-0.0246	-0.228	-6	-0.038	0	2.351	2.347
19	3.269	-0.2347	-0.0301	-0.204	-5.9	0.223	0	1.083	1.099

*Member of test set.
[a]Data obtained from eq. (1).

represent of the whole span. The semiempirical "rule of thumb" indicates that at least five or six data points should be present by descriptor [45]. In accordance to the total number of molecules (N=19), we think that a model with as maximum as two molecular descriptors is a suitable model.

The molecular descriptors: the dipole moment, E_{HOMO}, E_{LUMO}, GAP and ΔG_{bind} of LCM derivatives are listed in the Table **3**. These five descriptors were proposed assuming that they could have an important influence on the biological activity of LCM derivatives (for example, LUMO energy describes the electron-accepting character and is essential to understand the charge transfer processes that occur when a molecule interacts with biological receptors [33, 34, 46]; GAP describes the energy required for an intramolecular electron transfer, and it is related to polar reactivity, so, molecules with a low value of GAP could have an intramolecular electron transfer and are reactive species). However, a poor correlation of dependent variable (log$_{10}$ED$_{50}$) with these descriptors was found. The equations and the regression coefficients for each descriptor and the best models for the combination of two and three descriptors are shown in Table **4**. The E_{HOMO} descriptor showed highest correlation coefficient, R=0.352. The combination of two and three descriptors was also analyzed resulting in a maximum correlation coefficient of 0.411. The negative signs of the coefficient of E_{HOMO} indicate that this descriptor have an indirect relationship with the activity. Thus,

compounds with high E_{HOMO} values could be active species. Similarly, E_{HOMO} and E_{LUMO}, present in the three-descriptors equation (see Table **4**), show an indirect relationship with the log$_{10}$ED$_{50}$ values, while ΔG_{bind} have a positive contribution to the activity.

The low correlation presented by these molecular descriptors suggests that other descriptors require to be evaluated to interpret the biological activity of this family of compounds. Thus, we developed a QSAR model using the descriptors calculated with Dragon software. The minimum standard deviation (S) values of the generated models with one and two descriptors are presented in Table **5**. The excellent statistical data obtained in the calibration procedure, the cross validation and the external validation indicate the two-descriptor model has the highest predictive power. The mathematical equation is the following:

Log$_{10}$ED$_{50}$ = 2.144 (0.10) - 4.3581 (0.61) **MATS8p** + 1.5292 (0.20) **nCN**   (1)

N=15,   S=0.162,   R=0.957,   F=44.50,   CorrMax=0.237, S_{loo}=0.193, R_{loo}=0.900, $R_{l\%o}$=0.717, S^{rand}=0.24, R_{test}=0.839

where N is the number of molecules of the calibration set, F is the Fisher parameter, CorrMax represents the maximum intercorrelation coefficient between two descriptors of the model, test subindex applies to the test set, and rand supraindex stands for y-Randomization.

Table 4.   Lineal Models for Anticonvulsant Activity and Molecular Descriptors

Molecular Descriptors	Equation of Models	Correlation Coefficient
Dipole Moment (μ)	$Log_{10}ED_{50}=1.902-0.109*(\mu)$	0.161
HOMO energy (E_{HOMO})	$Log_{10}ED_{50}=-3.4-20.017*E_{HOMO}$	0.352
LUMO energy (E_{LUMO})	$Log_{10}ED_{50}=1.386-5.225*E_{LUMO}$	0.128
$\Delta E_{HOMO-LUMO}$ (GAP)	$Log_{10}ED_{50}=0.905-3.196*GAP$	0.098
Gibbs free energy binding (ΔG_{bind})	$Log_{10}ED_{50}=4.010+0.409*\Delta G_{bind}$	0.194
(μ)/E_{HOMO}	$Log_{10}ED_{50}=-3.01-0.097*(\mu) - 19.596*E_{HOMO}$	0.379
E_{HOMO}/E_{LUMO} /ΔG_{bind}	$Log_{10}ED_{50}=-1.310-18.801*E_{HOMO} -6.682*E_{LUMO}+ 0.343*\Delta G_{bind}$	0.411

Table 5.   The Best Models Containing One and Two Descriptors, d is the Numbers of Descriptors of Model, S is the Model's Standard Deviation, R is the Correlation Coefficient, Loo Subindex Belongs to the Leave-One-Out Cross-Validation Result

d	S	R	S_{loo}	R_{loo}	Descriptors Used	Description
1	0.404	0.662	0.446	0.573	X4A	Average connectivity Index Chi-4.
2	0.162	0.957	0.193	0.900	MATS8p	Moran autocorrelation of lag 8 weighted by atomic polarizabilities. descriptor
					nCN	Number of nitriles aliphatic.

The predicted $log_{10}ED_{50}$ values are shown in Table **3** while that predicted *vs* experimental $log_{10}ED_{50}$ plot is illustrated in the (Fig. (**3**), left). In the plot, the dotted lines represent the 20% difference from a perfect fit (about 2.5S). The molecule 6 exhibits > 2.5S in dispersing the residual, (Fig. (**3**), right), while the rest of molecules of test set present an error comparable to the calibration set. Since compound 6 lacks of structural differences which could allow explain the error in the predicted activity, we think that this error is related to the high MATS8p value of this compound which is out of the range of the model. Thus, the model does not allow the extrapolation of the data.

The absolute standardized regression coefficients for MATS8p and nCN descriptors are 0.725 and 0.763, respectively. The sign of the regression coefficients suggests that low predicted $log_{10}ED_{50}$ values (major activity) are obtained increasing MATS8p values and decreasing nCN values. Moran Autocorrelation of lag 8 weighted by atomic polarizabilities descriptor (MATS8p) is a 2D autocorrelation descriptor that describe how a considered property is distributed along a topological molecular structure. Molecules with substituents in R^2 as 4-OCF$_3$, 4-CH(CH$_3$)$_2$, 4-CH=CH$_2$ and 4-Cl have a high MATS8p value and they are most active compounds. In contrast, the molecules with low MATS8p values (4-CH$_2$OCH$_3$ as substituent) have a poor biological activity. Considering the substitution in R^1, molecules with CH$_2$OH and CH$_3$ have low MATS8p values and a poor activity. On the other hand, number of aliphatic nitriles (nCN) is a functional group descriptor and the presence of this functional group decreases the biological activity.

Analyzing 10000 cases of y-randomization, the smallest S value found (0.24) is larger than S_{cal} = 0.162, showing the model resulted in a real structure-activity relationship and is
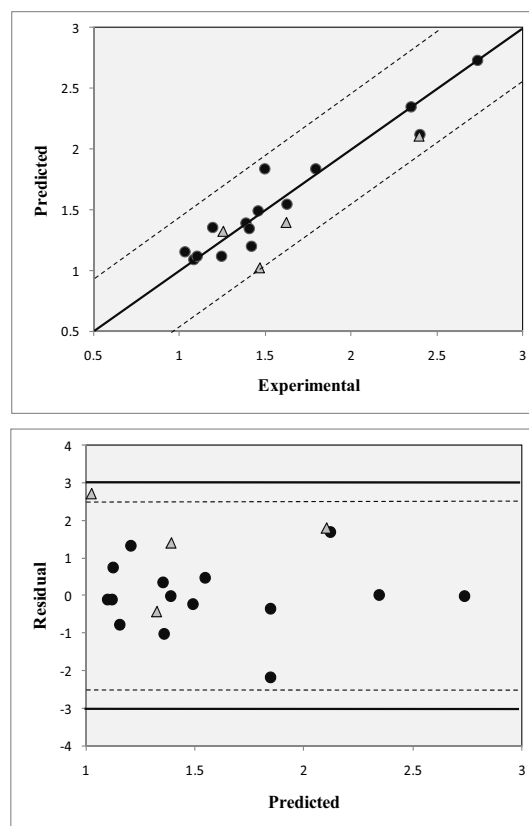

Fig. (3). Left: experimental versus predicted $Log_{10}ED_{50}$ for the calibration set (circles) and test set (triangles). The solid line represents a perfect correlation. The dotted lines represent ±20% difference from a perfect fit. Right: dispersion plot of the residuals for the calibration (circles) and test sets (triangles). The solid line represents 3S and dotted lines represent 2.5S.

not a fortuitous correlation. The results of theoretical validations show an excellent predictive capacity of the model. The correlation coefficients are: 0.900 (R_{loo}) and 0.717 ($R_{l\%o}$) for leave-one-out and leave-more-out cross-validation techniques, respectively. The correlation coefficient for external validation, R_{test}=0.839 indicate that model have a high power predicted for compounds external to calibration set.

This new model was developed using a minor number of compounds in relation to the obtained one in a previous work [22]. Fewer compounds contribute less information to the model delimiting the diversity of compounds that can be predicted correctly. However, we consider that model presents some advantages: the anticonvulsant activity of the used 18 LCM derivatives were determined in identical experimental conditions, the lower number of variables results in a simpler model, and finally, both descriptors consider only the 2D structure and are independent of the uncertainties associated to geometry optimization. Thus, the model can be used to predict the ED_{50} values of new candidate anticonvulsant drugs.

CONCLUSION

We report a detailed investigation on the molecular structure, docking into CA and structure-activity relationship of LCM and 18 LCM derivatives. According to the docking analysis, (R)-LCM and the 18 derivatives present high affinity to the active site of CA making favorable interactions with Thr200, Asn67, Gln92, and Phe131. The complexes show overall ΔG_{bind} values ranging from -6.6 to -5.5 kcal mol^{-1}. The mathematical equation shows a poor correlation between the ΔG_{bind} and the anticonvulsant activity (R<0.20). However, we developed an original two-descriptor QSAR model of high quality (R=0.957) and predictive power (R_{test}=0.839) which correlates two structural features (2D descriptors) of LCM derivatives with their anticonvulsant activity having advantages and disadvantages on the before developed model.

The results indicate that zinc-binding site of CA is, in fact, a target of LCM and LCM derivatives which have checked anticonvulsant activity. In addition, we provide important data about the relationship between the anticonvulsant activity and CA inhibition and, also, structural information can be used in the future for rational design of new anticonvulsant drugs.

CONFLICT OF INTEREST

The authors confirm that this article content has no conflict of interest.

ACKNOWLEDGEMENTS

SUPPLEMENTARY MATERIAL

Supplementary material is available on the publisher's web site along with the published article.

REFERENCES

[1] Perucca, E.; Yasothan, U.; Clincke, G.; Kirkpatrick, P. Lacosamide. *Nat. Rev. Drug. Discov.,* **2008**, *7*, 973-974.
[2] Höfler, J.; Trinka, E. Lacosamide as a new treatment option in status epilepticus. *Epilepsia*, **2013**, *54*, 393-404.
[3] Choi, D.; Stables, J.P.; Kohn, H. Synthesis and anticonvulsant activities of N-benzyl-2-acetamidopropionamide derivatives. *J. Med. Chem.*, **1996**, *39*, 1907-1916.
[4] Bardel, P.; Bolanos, A.; Kohn, H. Synthesis and anticonvulsant activities of a-Acetamido-N-benzylacetamide derivatives containing an electron-deficient a-heteroaromatic substituent. *J. Med. Chem.*, **1994**, *37*, 4567-4571.
[5] Kohn, H.; Sawhney, K.N.; Robertson, D.W.; Leander, J.D. Anticonvulsant properties of *N*-substituted α,α-diamino acid derivatives. *J. Pharm. Sci.*, **1994**, *83*, 689-691.
[6] Béguin, C.; LeTiran, A.; Stables, J.P.; Voyksnerc, R.D.; Kohn, H. *N*-Substituted amino acid *N'*-benzylamides: synthesis, anticonvulsant, and metabolic activities. *Bioorg. Med. Chem.*, **2004**, *12*, 3079-3096.
[7] Andurkar, S.V.; Stables, J.P.; Kohn, H. The anticonvulsant activities of *N*-benzyl 3-methoxypropionamides. *Bioorg. Med. Chem.,* **1999**, *7*, 2381-2389.
[8] Morieux, P.; Stables, J.P.; Kohn, H. Synthesis and anticonvulsant activities of *N*-benzyl (2*R*)-2-acetamido-3-oxysubstituted propionamide derivatives. *Bioorg. Med. Chem.,* **2008**, *16*, 8968-8975.
[9] Salomé, C.; Salomé-Grosjean, E.; Park, K.D., Morieux, P.; Swendiman, R.; DeMarco, E.; Stables, J.P.; Kohn, H. Synthesis and Anticonvulsant Activities of (*R*)-*N*-(4'-Substituted)benzyl 2-Acetamido-3-methoxypropionamides. *J. Med. Chem.,* **2010**, *53*, 1288-1305.
[10] Park, K.D.; Yang, X.F.; Lee, H.; Dustrude, E.T.; Wang, Y.; Khanna, R.; Kohn, H. Discovery of lacosamide affinity bait agents that exhibit potent voltage-gated sodium channel blocking properties. *ACS Chem. Neurosci.*, **2013**, *4*, 463-474.
[11] Niespodziany, I.; Leclère, N.; Vandenplas, C.; Foerch, P.; Wolff, C. Comparative study of lacosamide and classical sodium channel blocking antiepileptic drugs on sodium channel slow inactivation. *J. Neurosci. Res.*, **2013**, *91*, 436-443.
[12] Wang, Y.; Park, K.D.; Salomé, C.; Wilson, S.M.; Stables, J.P.; Liu, R.; Khanna, R.; Kohn, H. Development and characterization of novel derivatives of the antiepileptic drug lacosamide that exhibit far greater enhancement in slow inactivation of voltage-gated sodium channels. *ACS Chem. Neurosci.,* **2011**, *2*, 90-106.
[13] Temperini, C.; Innocenti, A.; Scozzafava, A.; Parkkila, S.; Supuran, C.T. The Coumarin-binding site in carbonic anhydrase accommodates structurally diverse inhibitors: the antiepileptic lacosamide as an example and lead molecule for novel classes of carbonic anhydrase inhibitors. *J. Med. Chem.*, **2010**, *53*, 850-854.
[14] Ekinci, D.; Kurbanoglu, N.I.; Salamcı, E.; Şentürk, M.; Supuran, C.T. Carbonic anhydrase inhibitors: inhibition of human and bovine isoenzymes by benzenesulphonamides, cyclitols and phenolic compounds. *J. Enzyme Inhib. Med. Chem.,* **2012**, *27*, 845-848.
[15] Supuran, C.T.; Scozzafava, A. Carbonic anhydrase inhibitors and their therapeutic potential. *Expert Opin. Ther. Pat.*, **2000**, *10*, 575-600.
[16] Supuran, C.T.; Scozzafava, A. Carbonic anhydrase inhibitors. *Curr. Med. Chem., Immunol. Endoc. Metab. Agents.*, **2001**, *1*, 61-97.
[17] Supuran, C.T.; Scozzafava, A.; Cassini, A. Carbonic anhydrase inhibitors. *Med. Res. Rev.*, **2003**, *23*, 146-189.
[18] Pastorekova, S.; Parkkila, S.; Pastorek, J.; Supuran, C.T. Carbonic anhydrases: current state of the art, therapeutic applications and future prospects. *J. Enzyme Inhib. Med. Chem.*, **2004**, *19*, 199-229.

[19]   Supuran, C.T. Carbonic anhydrases: novel therapeutic applications for inhibitors and activators. *Nat. Rev. Drug Discov.*, **2008**, *7*, 168-181.

[20]   Nishimori, I.; Vullo, D.; Innocenti, A.; Scozzafava, A.; Mastrolorenzo, A.; Supuran, C.T. Carbonic anhydrase inhibitors: Inhibition of the transmembrane isozyme XIV with sulfonamides. *Bioorg. Med. Chem. Lett.*, **2005**, *15*, 3828-3833.

[21]   Casini, A.; Antel, J.; Abbate, F.; Scozzafava, A.; David, S.; Waldeck, H.; Sch€afer, S.; Supuran, C.T. Carbonic anhydrase inhibitors: SAR and X-ray crystallographic study for the interaction of sugar sulfamates/sulfamides with isozymes I, II and IV. *Bioorg. Med. Chem. Lett.*, **2003**, *13*, 841-845.

[22]   Garro Martinez, J.C.; Duchowicz, P.R.; Estrada, M.R.; Castro, E. A multivariate qsar study on the anticonvulsant activity of acetamido-N-benzylacetamide derivatives. influence of different molecular descriptors. *MATCH Commun. Math. Comput. Chem.,* **2012***, 67*, 745-758.

[23]   Masereel, B.; Rolin, S.; Abbate, F.; Scozzafava, A.; Supuran, C.T. Carbonic anhydrase inhibitors: Anticonvulsant sulfonamides incorporating valproyl and other lipophilic moieties. *J. Med. Chem.*, **2000**, *45*, 312-320.

[24]   Dragon 3.0 Evaluation Version. Available online: http://www.disat.unimib.it/chm.

[25]   Hehre, W.J.; Ditchfield, R.; Pople, J.A. Self—consistent molecular orbital methods. XII. Further extensions of gaussian—type basis sets for use in molecular orbital studies of organic molecules. *J. Chem. Phys.*, **1972**, *56*, 2257-2261.

[26]   Becke, A.D. Density-functional thermochemistry. III. The role of exact exchange. *J. Chem. Phys.*, **1993**, *98*, 5648-5653.

[27]   Lee, C.; Yang, W.; Parr, R.G. Development of the Colle-Salvetti correlation-energy formula into a functional of the electron density. *Phys. Rev. B*., **1988**, *37*, 785-789.

[28]   Cancès, E.; Mennucci, B.; Tomasi, J. A new integral equation formalism for the polarizable continuum model: Theoretical background and applications to isotropic and anisotropic dielectrics. *J. Chem. Phys.*, **1997**, *107*, 3032-3041.

[29]   Miertus, S.; Scrocco, E.; Tomasi, E. Electrostatic interaction of a solute with a continuum. A direct utilization of *ab initio* molecular potentials for the prevision of solvent effects. *J. Chem. Phys.*, **1981**, *55,* 117-129.

[30]   Frisch, M.J.; Trucks, G.W.; Schlegel, H.B.; Scuseria, G.E.; Robb, M.A.; Cheeseman, J.R.; Scalmani, G.; Barone, V.; Mennucci, B.; Petersson, G.A.; Nakatsuji, H.; Caricato, M.; Li, X.; Hratchian, H.P.; Izmaylov, A.F.; Bloino, J.; Zheng, G.; Sonnenberg, J.L.; Hada, M.; Ehara, M.; Toyota, K.; Fukuda, R.; Hasegawa, J.; Ishida, M.; Nakajima, T.; Honda, Y.; Kitao, O.; Nakai, H.; Vreven, T.; Montgomery, Jr., J.A.; Peralta, J.E.; Ogliaro, F.; Bearpark, M.; Heyd, J.J.; Brothers, E.; Kudin, K.N.; Staroverov, V.N.; Keith, T.; Kobayashi, R.; Normand, J.; Raghavachari, K.; Rendell, A.; Burant, J.C.; Iyengar, S.S.; Tomasi, J.; Cossi, M.; Rega, N.; Millam, V; Klene, M.; Knox, J.E.; Cross, J.B.; Bakken, V.; Adamo, C.; Jaramillo, J.; Gomperts, R.; Stratmann, R.E.; Yazyev, O.; Austin, A.J.; Cammi, R.; Pomelli, C.; Ochterski, J.W.; Martin, R.L.; Morokuma, K.; Zakrzewski, V.G.; Voth, G.A.; Salvador, P.; Dannenberg, J.J.; Dapprich, S.; Daniels, A.D.; Farkas, O.; Foresman, J.B.; Ortiz, J.V.; Cioslowski, J. and Fox, D.J. *Gaussian 09,* Revision C.01; Gaussian, Inc.: Wallingford CT, **2010**.

[31]   Trott, O.; Olson, A.J. AutoDock Vina: improving the speed and accuracy of docking with a new scoring function, efficient optimization and multithreading. *J. Comput. Chem.*, **2010**, *31*, 455-461.

[32]   Bernstein, F.C.; Koetzle, T.F.; Williams, G.J.B.; Jr. Meyer, E.F.; Brice, M.D.; Rodgers, J.R.; Kennard, O.; Shimanouchi, T.; Tasumi, M. The protein data bank: A computer-based archival file for macromolecular structures. *J. Mol. Biol.*, **1977**, *112*, 535-542.

[33]   Putz, M.V. Residual-QSAR implications for genotoxic carcinogénesis. *Chem. Central J.,* **2011**, *5*, 29.

[34]   Putz M.V.; Lacrămă A.M. Introducing spectral structure activity relationship (S-SAR) analysis. Application to ecotoxicology. *Int. J. Mol. Sci*., **2007**, *8*, 363-391.

[35]   Putz M.V.; Dudaş N.A. Determining chemical reactivity driving biological activity from SMILES transformations: The bonding mechanism of anti-HIV pyrimidines. *Molecules*, **2013**, *18*, 9061-9116.

[36]   Todeschini, R.; Consonni, V. *Handbook of Molecular Descriptors*; Wiley-VCH: Weinheim, Germany, **2000**.

[37]   Garro Martinez, J.C.; Duchowicz, P.R.; Estrada, M.R.; Zamarbide, G.N.; Castro, E. Anticonvulsant activity of ringed enaminones: A QSAR study. *QSAR Comb. Sci*., **2009**, *28*, 1376-1385.

[38]   Garro Martinez, J.C.; Duchowicz, P.R.; Estrada, M.R.; Zamarbide, G.N.; Castro, E. QSAR Study and molecular design of open-chain enaminones as anticonvulsant agents. *Int. J. Mol. Sci.,* **2011**, *12*, 9354-9368.

[39]   Duchowicz, P.R.; Castro, E.A.; Fernández, F.M.; González, M.P. A new search algorithm of QSPR/QSAR theories: Normal boiling points of some organic molecules. *Chem. Phys. Lett*., **2005**, *412*, 376-380.

[40]   Duchowicz, P.R.; Castro, E.A.; Fernández, F.M. Alternative algorithm for the search of an optimal set of descriptors in QSAR-QSPR studies. *MATCH Commun. Math. Comput. Chem.*, **2006**, *55*, 179-192.

[41]   Wold, S.; Eriksson, L. *Chemometrics Methods in Molecular Design.* Wiley-VCH: Weinheim, Germany, **1995**.

[42]   Matlab 7.0. The MathWorks Inc. Natick, MA: USA, **2004**.

[43]   Alterio, V.; Di Fiore, A.; D'Ambrosio, K.; Supuran, C.T.; De Simone, G. X-Ray crystallography of CA inhibitors and its importance in drug design. In: *Drug design of zinc-enzyme inhibitors: functional, structural, and disease applications*; Supuran, C.T.; Winum, J.Y. (Eds.) Wiley: Hoboken, **2009**; pp. 73-138.

[44]   D'Ambrosio, K.; Vitale, R.M.; Dogne, J.M.; Masereel, B.; Innocenti, A.; Scozzafava, A.; De Simone, G.; Supuran, C.T. Carbonic anhydrase inhibitors: bioreductive nitro-containing sulfonamides with selectivity for targeting the tumor associated isoforms IX and XII. *J. Med. Chem*., **2008**, *51*, 3230-3237.

[45]   Hansch, C. *Comprehensive Drug Design*. Pergamon Press: New York, **1990**.

[46]   Honorio, K.M.; da Silva, A.B. An AM1 study on the electron-donating and electron-accepting character of biomolecules. *Int. J. Quantum Chem.*, **2003**, *95*, 126-132.